MODELING THE EFFECT OF ANCHOR GEOMETRY ON THE QUALITY FACTOR OF BULK MODE RESONATORS

Dustin D. Gerrard, Eldwin J. Ng, Chae H. Ahn, Vu A. Hong, Yushi Yang, and Thomas W. Kenny
Department of Mechanical Engineering, Stanford, CA, USA

ABSTRACT

High quality factor (Q) resonators are desired for numerous applications such as clocks and gyroscopes. For bulk acoustic wave resonators, energy dissipation through the anchors (i.e. anchor loss or anchor damping) can often limit Q. This work explores several designs of anchor geometries for a width extensional resonator with experimental results confirming that the geometry of the anchor can have a large effect on the mode shape as well as the quality factor. We present a Perfectly Matched Layer (PML) COMSOL model which is able to predict Q for several anchor loss limited anchor designs. Temperature dependencies of f and Q are also reported and favorable designs are set forth.

KEYWORDS

Anchor Loss, Bulk Mode Resonator, Perfectly Matched Layer, PML, Wave Dissipation.

INTRODUCTION

Energy losses through the anchor have been noted to be significant for both flexural and bulk mode resonators, with a number of models developed, from analytical [1] to finite elements [2-5]. These works demonstrate that the design of the anchor geometry is crucial for attaining high Qs when other energy loss mechanisms have been minimized. Several anchor designs are hence experimentally investigated here. We provide evidence that the Q is limited by anchor loss in some of these designs. Additionally we present a perfectly matched layer (PML) model used to simulate the anchor dissipation in these resonators. We see that there is good agreement between simulated and experimental values of Q for most of the devices. For some of the devices, it is possible that another damping mechanism – possibly Akheizer damping, is playing a role.

Bar Resonator and Anchor Designs

A promising resonator for the study of anchor dissipation is the width extensional resonator, as demonstrated in [6]. Three different anchor types are investigated (Fig. 1). The first is a secondary length extensional bar at both ends of the resonator supported in the middle, with a length equal to the dimension of the main resonant mode (X4 and X6). The second anchor type is a simple 6 × (3 or 5) µm bar B3 and B5. The final design is a T-shaped anchor that is designed to flex with Poisson effects of the main resonant mode [7].

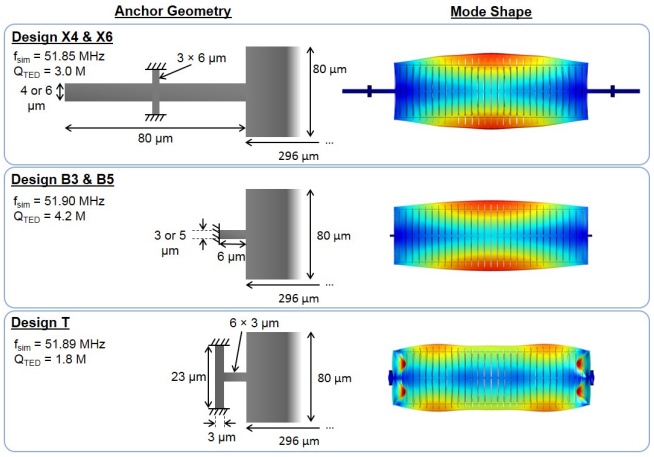

Figure 1: Anchor designs for the width extensional resonator with etch slots and their corresponding mode shapes. The colors from blue to red indicate zero to maximum displacement.

Mode shapes as simulated in COMSOL are distorted from the ideal width extensional mode reported in [6], in part due to the required etch slots dictated by the *epi-seal* encapsulation process for device release [8], and also by the anchor geometry (Fig. 1), which is analyzed here.

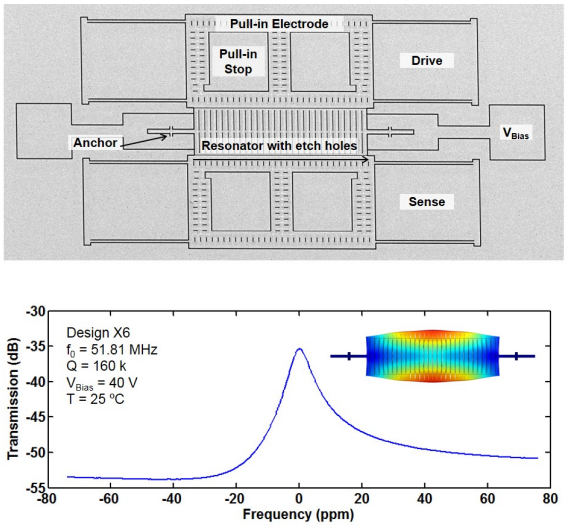

Figure 2: (Top) An SEM image of the device layer geometry before encapsulation. (Bottom) A frequency sweep of the resonator.

EXPERIMENTAL RESULTS

Width extensional resonators at 52 MHz were fabricated in the *epi-seal* encapsulation process [8] on 4 × 10^{18} cm^{-3} boron-doped silicon. Pull-in drive/sense electrodes were used to decrease the gap size and hence motional impedance [9]. The device structure prior to encapsulation as well as the measured frequency sweep for the X6 design is shown in Fig. 2. Simulated and experimental frequencies match within 0.1% (Fig. 3), with frequency-temperature dependences predicted to within 100 ppm.

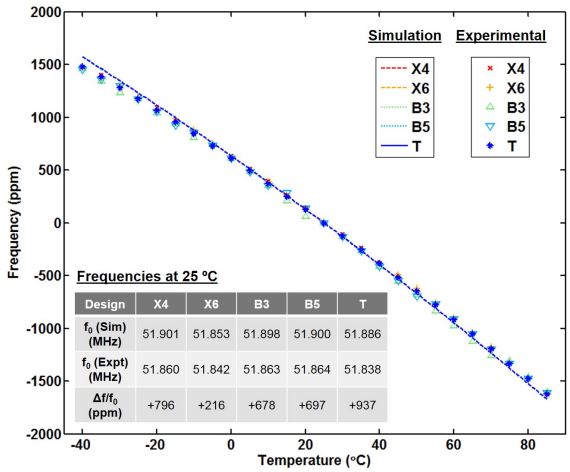

Design	X4	X6	B3	B5	T
f_0 (Sim) (MHz)	51.901	51.853	51.898	51.900	51.886
f_0 (Expt) (MHz)	51.860	51.842	51.863	51.864	51.838
$\Delta f/f_0$ (ppm)	+796	+216	+678	+697	+937

Figure 3: Frequency-temperature dependences demonstrating similar dependences for all anchor geometries.

Qs were measured using ringdown as temperature instability (± 1ºC) is seen to cause narrowing/widening of the frequency sweep peak especially for high Q resonators, and can result in inaccurate Q values. The measured Qs for these resonators (Fig. 4) are between 20 and 180 k depending on anchor design, and are seen to be over an order of magnitude lower than the simulated thermoelastic dissipation Q_{TED} and show no correlation in terms of design or temperature dependence. Less than 5% of the measured Q can hence be attributed to Q_{TED}. A simulation of gas damping Q_{Gas} with pressure of 1 Pa using a finite element implementation of Bao's squeeze film model [9] gave Q_{Gas} values in excess of 30e6. The Akhieser damping limit ($f \times Q_{AKE}$) has been reported to be around 2e13 Hz for silicon, which the X4 and X6 designs are close to at ~8e12 Hz [10].

Anchor designs B3, B5, and T are thus clearly anchor dissipation limited and exhibit the expected temperature independence. The X anchor geometry is seen in Fig. 5 to operate as a secondary length extensional resonator that couples to the main resonator via the Poisson effect, acting as a mechanical step-down gear. With reduced displacements in the secondary resonator, the better anchor isolation results in a Q_{Anchor} that is more than twice as large as that of the B or T anchors.

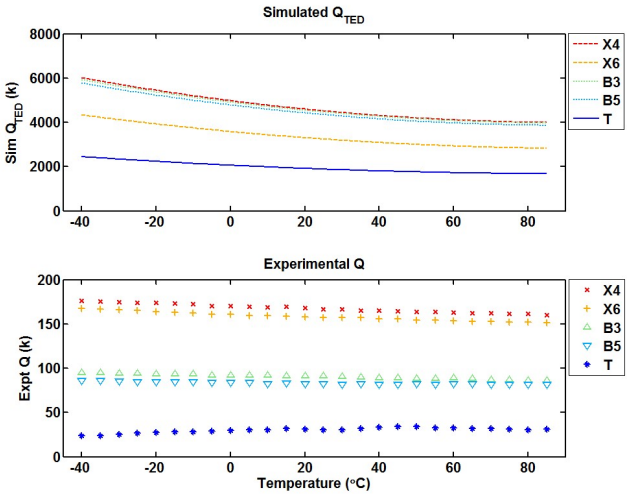

Figure 4: (Top) Simulated TED quality factors and (bottom) experimental quality factors showing large discrepancies and no correlation in temperature or design, suggesting that these devices are not TED limited.

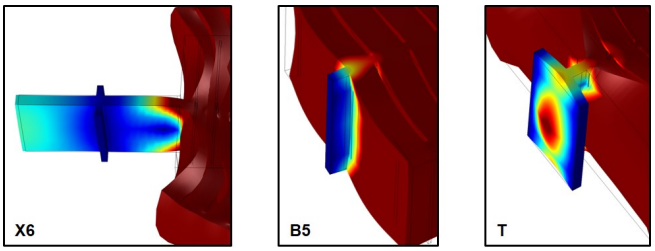

Figure 5: Zoomed-in displacement plots of the mode shapes of the various anchors at resonance. Colors have been scaled to magnify the displacements in the anchor.

PERFECTLY MATCHED LAYER MODEL

Because it is not possible to model the full substrate, PMLs are often used to quantify anchor loss in MEMS resonators using a finite element model [11, 12]. The PML serves as an artificial boundary layer with the functionality of a semi-infinite space that absorbs acoustic wave energy from the resonating MEMS device. Ideally the PML prevents all waves from being reflected back into the MEMS resonator [2, 13]. In this study we use the PML definition in COMSOL to model the semi-infinite substrate. COMSOL uses the method of stretched coordinates to damp acoustic waves traveling perpendicularly to the PML-device interface. We quantify the energy lost in the PML and are able to calculate anchor loss Q.

PML Parameter Variation

In order to decrease computation time we apply three-way symmetry to each device, and thus only model one-eighth of the device. Each anchor is attached to a quarter-sphere (i.e. wedge) of anisotropic silicon substrate interface region. Outside of this substrate layer is a spherical wedge PML (see Fig. 6). The wavelength is the speed of sound in silicon divided by frequency.

$$8433\ \mathrm{m{\cdot}s^{-1}} / 51.9\ \mathrm{MHz} = 162\ \mu\mathrm{m} \quad (1)$$

The lengths of the PML radius and the interface region radius are critical to obtaining an accurate estimation of Q [3, 4]. We choose the dimensions of the interface layer and PML to be on the same order of magnitude as the wavelength (elaborated below). Furthermore, the material properties of the PML, interface region, and device are those of anisotropic silicon crystal.

In all three types of anchors we fix the external boundary of the PML. Figure 6 illustrates the substrate, PML, and device regions with three-way symmetry. Also, two zoomed-in views of anchors T and X are provided.

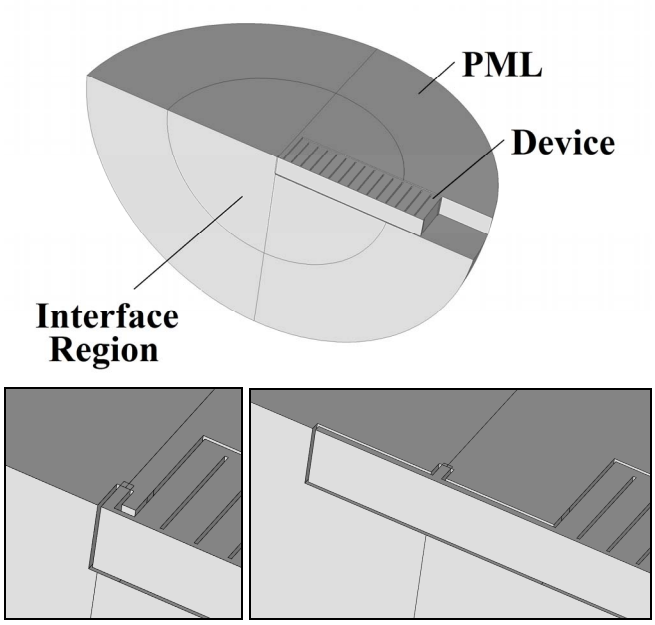

Figure 6: Top: PML wedge, substrate, and device in COMSOL, B anchor type. Bottom Left: T anchor geometry in COMSOL. Bottom Right: X anchor type in COMSOL.

The simulated Q is highly dependent on the dimensions of the PML and the scaling factor (α), and thus it is essential to determine appropriate values. The parameter α is used to linearly scale the coordinates when using a stretched coordinates PML model and is built into the COMSOL PML definition. One method of selecting appropriate PML parameters, as suggested in [4], is to vary the dimensions until values are obtained which give a Q that matches the analytical values of Q for various modes of an anchored beam [1]. In our case we vary the inner radius of the PML and choose a value which minimizes Q. We see that varying the outer radius has little influence on the Q. We then choose α by taking the one which gives a minimum value of Q [4] (see Fig. 7).

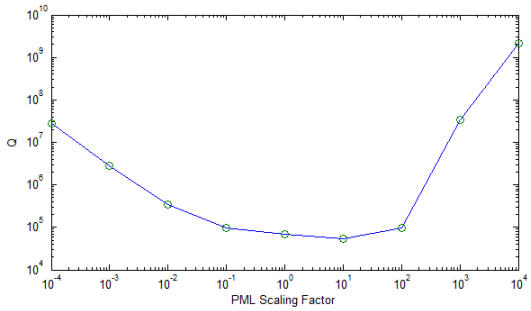

Figure 7: Q as a function of PML scaling factor for B3 anchor. The minimum Q occurs with a scaling factor of 10 which is the parameter used as in [4]. The minimum Q is reported in Fig 9.

PML Meshing Parameters

To capture all waves we use at least five elements per wavelength in the PML simulation [3]. The PML is meshed using tetrahedrons. The interface region and device are also meshed using finer tetrahedrons (see Fig. 8).

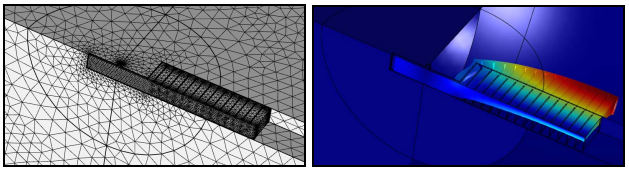

Figure 8: Left: Hemispherical PML meshed with swept trigonal prisms and eighth or bar resonator tetrahedral meshed. Anchor type X. Right: Width extensional mode for anchor B.

RESULTS AND DISCUSSION

After varying the radii of the interface region and PML to obtain an appropriate values we tune the PML scaling factor. For devices T, B3, and B5 we are able to develop a PML model that agrees well with experimental results (see Table. 1). The simulated values of Q are no more than 6.5% different from the experimental Qs. This small residual difference can be accounted for from differences in the dimensions, aberrations in the fabricated devices and simple measurement error. Other loss mechanisms including gas damping and Akhiezer play a small role in the energy loss for this device, as the F*Q products for these devices are well below the Akheizer limit, and gas damping would have a strong temperature dependence.

For the devices X4 and X6 we were not able to obtain good agreement – the predictions for anchor damping from our method exceed the measurements by a factor of around 5X for both devices. It is possible that there are other damping mechanisms beginning to play a role in the behavior of this device. For example, the higher F*Q product associated with the X4 and X6 devices could indicate that Akheizer damping is beginning to play a role, causing the total measured Q to be less than the Q expected just from anchor damping in these devices. Based on our results, and on the large uncertainty in the exact amplitude

of Akheizer damping, we cannot be sure if it is important or not for these devices.

Table1: PML modeled anchor dissipation Q vs. simulated Q-TED vs. experimental.

	Q_TED	Q_anchor	Q_sim_tot	Q_exp
T	2.21E+06	3.21E+04	3.17E+04	3.03E+04
B3	5.15E+06	8.79E+04	8.64E+04	9.09E+04
B5	4.66E+06	7.86E+04	7.73E+04	8.25E+04
X4	5.37E+06	1.16E+06	9.52E+05	1.67E+05
X6	3.87E+06	1.11E+06	8.63E+05	1.57E+05

We see good agreement between the experimental and simulated models the values of Q for anchor geometries T, and B, but not for X. It is possible that a more accurate simulation may be constructed by modeling the bar resonator in greater detail by including the oxide and cap layers in the PML simulation.

Since dimensions of the PML can affect the simulated value of Q [4], more work will be done to investigate how each of the parameters including PML size, scaling factor, mesh geometry, etc. in COMSOL affect Q and how these parameters can be independently constrained for a general anchor loss model. This will allow us to determine how to more accurately predict anchor loss Q for a general MEMS device.

CONCLUSION

In this paper we have demonstrated that anchor loss is the limiting energy loss mechanism in several of our width-extensional bar resonators. Evidence of this is the measured Q is essentially invariant over a range of temperature from -40ºC to 85ºC and is a couple orders of magnitude below the simulated Q_{TED}. Furthermore, we provided a COMSOL simulation model with PML that calculates a Q which agrees with our experimental results to within 6.5% for several of these devices.

Further modeling and validation of anchor loss models will provide insight into accurate quantification of anchor loss Q via finite element modeling. Insight into how wave energy is dissipated through anchor will allow us to design high-Q MEMS resonators.

ACKNOWLEDGEMENTS

This work was supported by the Defense Advanced Research Projects Agency (DARPA) Precision Navigation and Timing program (PNT) managed by Dr. Andrei Shkel and Dr. Robert Lutwak under contract # N66001-12-1-4260. The fabrication work was performed at the Stanford Nanofabrication Facility (SNF) which was supported by National Science Foundation through the NNIN under Grant ECS- 9731293.

REFERENCES:

[1] Z. L. Hao, A. Erbil, and F. Ayazi, "An analytical model for support loss in micromachined beam resonators with in-plane flexural vibrations," Sensors and Actuators a-Physical, vol. 109, pp. 156-164, Dec 1 2003.

[2] P. G. Steeneken, J. Ruigork, S. Kang, J. van Beek, J. Bontemps, and J. J. Koning, "Parameter Extraction and Support-Loss in MEMS Resonators," COMSOL Users Conference 2007, Grenoble, 2007.

[3] A. Frangi, A. Bugada, M. Martello, and P. T. Savadkoohi, "Validation of PML-based models for the evaluation of anchor dissipation in MEMS resonators," European Journal of Mechanics a-Solids, vol. 37, pp. 256-265, Jan-Feb 2013.

[4] V. Thakar and M. Rais-Zadeh, "Optimization of tether geometry to achieve low anchor loss in Lamé mode resonators," IEEE International Frequency Control Symposium 2013, pp. 129-132, July 2013.

[5] J. Segovia-Fernandez, M. Cremonesi, C. Cassella, A. Frangi, and G. Piazza, "Anchor Losses in AlN Contour Mode Resonators," Microelectromechanical Systems, Journal of, vol. 24, pp. 265-275, 2015.

[6] S. Pourkamali, G. K. Ho, and F. Ayazi, "Low-impedance VHF and UHF capacitive silicon bulk acoustic wave resonators - Part I: Concept and fabrication," IEEE Transactions on Electron Devices, vol. 54, pp. 2017-2023, Aug 2007.

[7] L. Khine and M. Palaniapan, "7MHZ length-extensional soi resonators with T-shaped anchors," Solid-State Sensors, Actuators and Microsystems Conference (Transducers) 2009, pp. 1441-1444, June 2009.

[8] A. Partridge and M. Lutz, "Episeal pressure sensor and method for making an episeal pressure sensor," U.S. Patent 6928879, 2005.

[9] E. J. Ng, Y. Yang, V. A. Hong, C. H. Ahn, D. L. Christensen, B. A. Gibson, et al., "Stable Pull-in Electrodes for Narrow Gap Actuation," IEEE International Conference on Micro Electro Mechanical Systems (MEMS) 2014, pp. 1281-1284, 2014.

[10] M. H. Bao, H. Yang, H. Yin, and Y. C. Sun, "Energy transfer model for squeeze-film air damping in low vacuum," Journal of Micromechanics and Microengineering, vol. 12, pp. 341-346, May 2002.

[11] Y.H. Park, K. C. Park. "High-fidelity modeling of MEMS resonators. Part I. Anchor loss mechanisms through substrate." Journal of Microelectromechanical Systems, 13.2: 238-247, 2004.

[12] Y. H. Park, and K. C. Park. "High-fidelity modeling of MEMS resonators. Part II. coupled beam-substrate dynamics and validation." Journal of Microelectromechanical Systems, 13.2: 248-257, 2004.

[13] D. S. Bindel, Emmanuel Quevy, T. Koyama, S. Govindjee, J. W. Demmel, and R. T. Howe, "Anchor Loss Simulation in Resonators," IEEE International Conference on Micro Electro Mechanical Systems (MEMS) 2005, pp. 133-136, 30 Jan.-3 Feb. 2005 2005.